Journal of Biotechnology 168 (2013) 584–588

Contents lists available at ScienceDirect

Journal of Biotechnology

journal homepage: www.elsevier.com/locate/jbiotec

Short communication

Wafer-scale nanowell array patterning based electrochemical impedimetric immunosensor

JuKyung Lee[a,1], SiHyeong Cho[b,1], JungHwan Lee[b], HeonYul Ryu[b], JinGoo Park[b,c], SunHee Lim[d], ByungDo Oh[d], ChangWoo Lee[e], Wilber Huang[f], Ahmed Busnaina[a], HeaYeon Lee[a,*]

[a] Department of Mechanical and Industrial Engineering, College of Engineering, Northeastern University, Boston, MA 02115, USA
[b] Department of Bionano Technology, Hanyang University, Ansan 426-791, South Korea
[c] Department of Materials Engineering, Hanyang University, Ansan 426-791, South Korea
[d] All Medicus Co., Ltd., Anyang 431-062, South Korea
[e] Battelle-Korea, Korea University, Seoul 136-713, South Korea
[f] Abnova Co., Jhouzih St., Neihu District, Taipei City 114, Taiwan

ARTICLE INFO

Article history:
Received 6 May 2013
Received in revised form 9 August 2013
Accepted 22 August 2013
Available online 6 September 2013

Keywords:
Nanowell arrays (NWA) immunosensor
Wafer-scale nanopatterning
Electrochemical impedance spectroscopy (EIS)
Stress-induced-phosphoprotein-1 (STIP-1)

ABSTRACT

We have reported that nanowell array (NWA) can enhance electrochemical detection of molecular binding events by controlling the binding sites of the captured molecules. Using NWA biosensor based amperometric analysis, we have detected biological macromolecules such as DNA, protein or aptamers at low concentrations. In this research, we developed an impedimetric immunosensor based on wafer-scale NWA for electrochemical detection of stress-induced-phosphoprotein-1 (STIP-1). In order to develop NWA sensor through the cost-effective combination of high-throughput nanopattern, the NWA electrode was fabricated on Si wafer by krypton-fluoride (KrF) stepper semiconductor process. Finally, 12,500,000 ea nanowell with a 500 nm diameter was fabricated on 4 mm × 2 mm substrate. Next, by using these electrodes, we measured impedance to quantify antigen binding to the immunoaffinity layer. The limit of detection (LOD) of the NWA was improved about 100-fold compared to milli-sized electrodes (4 mm × 2 mm) without an NWA. These results suggest that wafer-scale NWA immunosensor will be useful for biosensing applications because their interface response is appropriate for detecting molecular binding events.

1. Introduction

Electrochemical impedance spectroscopy (EIS) is commonly used for label-free detection of analytes such a proteins, DNA and peptide. EIS based immunosensors have high sensitivity and are relatively simple to operate in comparison to other immunological methods that involve optical or piezoelectric instrumentation. Several reports have already demonstrated that impedimetric biosensors have favorable sensitivity, reliability, simplicity and ability to preserve the integrity the measured analyte (Chen et al., 2010; Daniels and Pourmand, 2007; Diouani et al., 2008; Hanien et al., 2008; Mathebula et al., 2009; Primiceri et al., 2009; Yu et al., 2006).

EIS-based immunosensors typically utilize antigen–antibody immunolayers that are very thin and have low electric permittivity. Molecular binding is detected by interruption of the faradaic current at the electrode, which generate an impedance signal (Berggren et al., 2001). In impedance system, we measure the change in impedance at the electrode interface at the double layer and in solution. Binding of the antigen to the antibody layer on the electrode prevents the redox probe from effectively transferring electrons to the electrode surface which induces changes in the double-layer capacitance and charge-transfer resistance of the electrode. As a result, EIS can transduce these electrode boundary phenomena to electric signals. Thus binding of specific antigens can be measured based on the impedance signal (Hause et al., 1981; Felice et al., 1992; Felice and Valentinuzzi, 1999).

In this study, we developed an highly sensitive immunosensor for quantitative detection of stress-induced-phosphoprotein-1 [STIP-1] using wafer-scale nanowell array (NWA) electrodes. In our previous work, we optimized NWA electrode based amperometric detection of molecular binding events by controlling the molecular binding sites (Kim et al., 2005a,b; Lee et al., 2006; Kim et al., 2008). Here, we used EIS with our NWA to detect antigens with low concentrations.

* Corresponding author. Tel.: +1 617 373 6165; fax: +1 617 373 6163.
E-mail address: he.lee@neu.edu (H. Lee).
[1] These authors contributed equally to this work.

0168-1656/$ – see front matter © 2013 Elsevier B.V. All rights reserved.
http://dx.doi.org/10.1016/j.jbiotec.2013.08.029

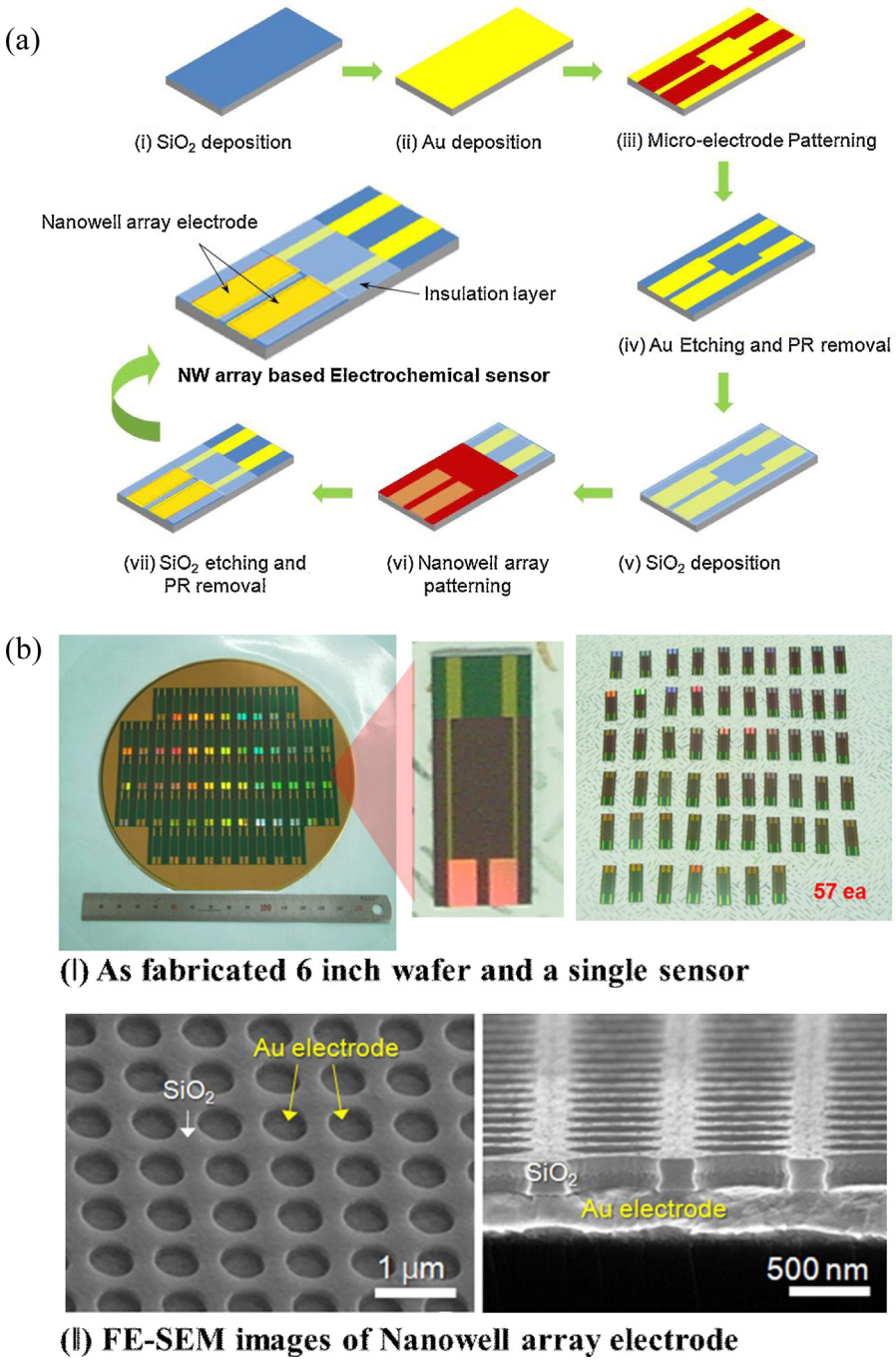

Fig. 1. Fabrication of NWA based electrochemical sensor. (a) Simple and high throughput nano-process for industrial application. (b) Photograph of as-fabricated samples (top) and SEM images of NWA electrode (bottom).

In general, e-beam lithography (EBL), nanoimprint lithography (NIL) and nanosphere lithography (NSL) are capable of creating nanopatterns that can be used to fabricate NWA. But these methods have low throughput and are limited to small areas. Therefore, in this study, we used a krypton-fluoride (KrF) stepper semiconductor process with a wavelength of 248 nm for the fabrication of NWA electrodes on 6-inch wafer. This wafer-scale fabrication method of nanopatterns has rapid, high-throughput and is highly reliable for the fabrication of NWA biosensor. The function of the wafer-scale NWA based impedimetric immunosensor was demonstrated by detecting STIP-1, which is biomarker for ovarian cancer biomarker (Wang et al., 2010).

2. Materials and methods

2.1. Wafer-scale NWA patterning method

A KrF stepper (PAS 5500/300C, ASML, Netherlands) was used for nanoscale patterning of NWA sensor on 6-inch wafer after PR coating as shown in Fig. 1(a). A 6-inch Si wafer was pre-cleaned using SPM (sulfuric peroxide mixture, H_2SO_4:H_2O_2 = 4:1) and diluted HF (DIW:HF = 100:1) to remove the organic contaminants and native oxide layer on the substrate, respectively. A 300 nm-thick silicon dioxide (SiO_2) layer was deposited on the Si substrate by plasma-enhanced chemical vapor deposition (PECVD, Plasma lab

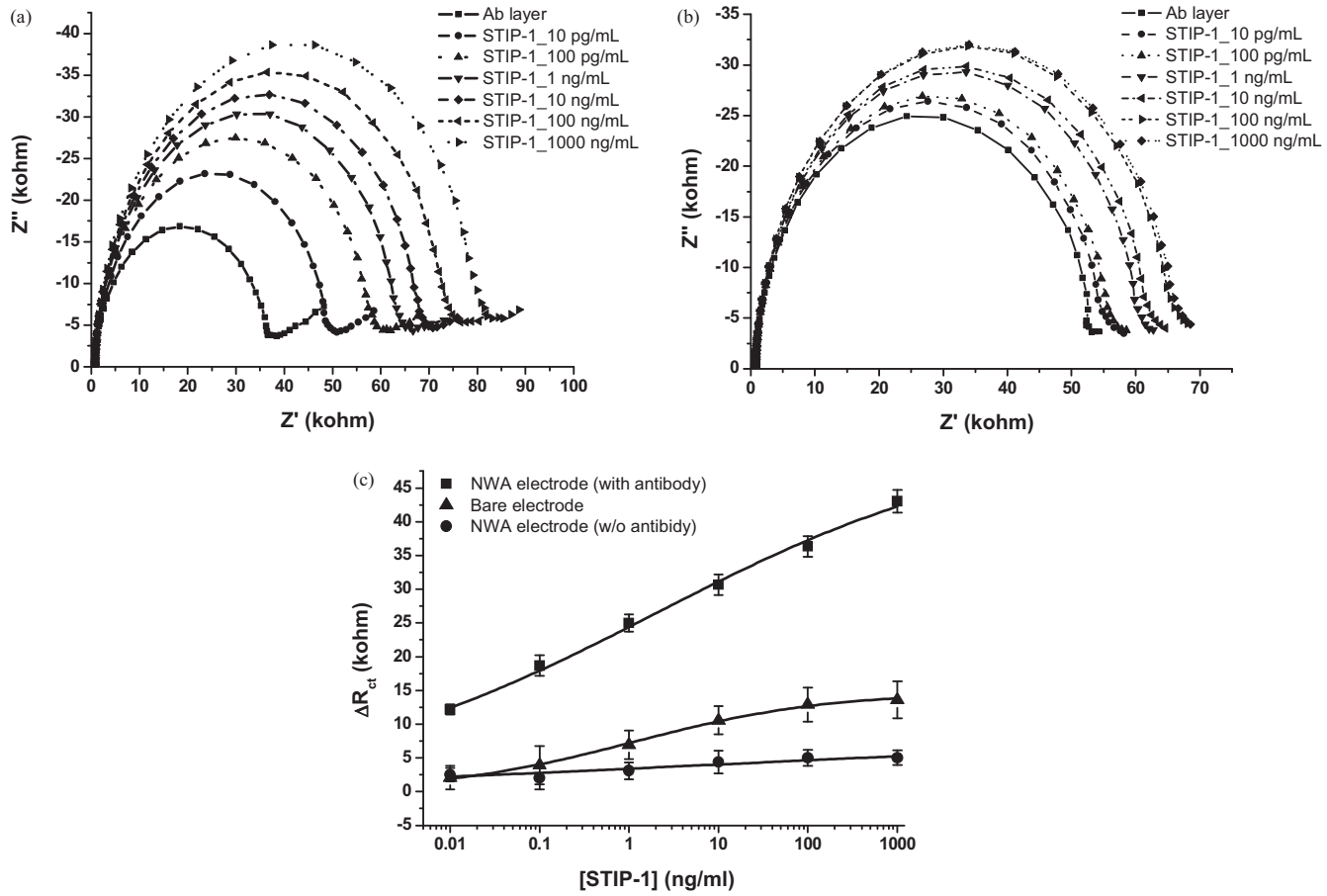

Fig. 2. EIS for binding of STIP-1 to the immunolayer on the electrodes. (a) Nyquist plot for the NWA electrode. (b) Nyquist plot for the bare electrode. (c) Quantitative analysis of STIP-1 and anti-STIP-1 antibody binding. Biotinylated anti-STIP-1 antibody layer was labeled with streptavidin on the NWA and bare electrodes. Error bars represent the standard deviations of three measurements. The applied potential was set to 50 mV against an Ag/AgCl reference electrode. The frequency range was 0.1 Hz to 1 MHz.

80Plus, Oxford, UK). A 30 nm-thin titanium adhesion layer and a 300 nm-thick gold electrode layer were deposited by sputtering (SRN-120, Sorona, Korea). After micro-patterning, the Ti/Au layers were etched in an inductively coupled plasma (ICP) etcher (Multiplex ICP, STS, UK). Photoresist (PR) was removed using a microwave asher (Enviro II, ULVAC, USA). A second SiO_2 layer with a thickness of 200 nm was deposited onto the Au layer using PECVD to pattern the NWA. The SiO_2 defined the array pattern and also served as an insulating layer. Finally, the exposed SiO_2 areas were etched using an ICP etcher (ICP380, Oxford, UK), and the PR was removed. The features of the large-area NWA electrodes were observed using field emission scanning electron microscopy (FE-SEM, S-4800, Hitachi, Japan) with an acceleration voltage of 15 kV.

2.2. Preparation of the immunoaffinity layer

Stress-induced-phosphoprotein-1 (STIP-1) and biotinylated anti-STIP-1 antibody were provided from Abnova (Taipei city, Taiwan). Streptavidin, ethanolamine hydrochloride, 11-mercapto undecanoic acid (11-MUA), N-(3-dimethylaminopropyl)-N′-ethylcarbodiimide (EDC), N-hydroxysuccinimide (NHS) and all other chemicals of analytical grade were purchased from Sigma–Aldrich (St. Louis, USA).

All electrodes were treated with aceton and cleaned with ethanol and DI water before use. After drying in a stream of N_2, self-assembled monolayers (SAMs) were prepared on the NWA electrodes by incubating the electrodes in 10 mM 11-mercaptoundecanoic acid dissolved in anhydrous ethanol for 1 h at room temperature. Next, 50 mM EDC and 50 mM NHS in pH 5.5 sodium acetate buffer were used to activate the ester functional froups. Streptavidin (10 μg/mL in PBS) was then immobilized on the SAMs for 30 min at room temperature. The unreacted functional ester groups were blocked with 1 M ethanolamine for 30 min. Finally, a solution of 10 μg/mL biotinylated anti-STIP-1 antibody was immobilized by biotin-streptavidin-affinity.

2.3. Electrochemical Impedimetric characterization

EIS was performed in 5 mM $K_3Fe(CN)_6$ in pH 7.4 PBS buffer as an electrolyte solution at room temperature using a potentiostat/galvanostat from IVIUM Co (Netherlands). The impedance spectra were recorded from 1 MHz to 0.1 Hz at 50 mV ac signal amplitudes. And DC potential is same as the open circuit potential. Each decade of frequency contained 10 points. For a total of 71 measurement points. After impedance measurement, data were fitted by using Z-view software. A glass Ag/AgCl reference electrode (diameter 6 mm, length 5 cm) a Pt counter electrode from BAS analytical instruments (West Lafayette, USA) and the NWA electrode were placed in an electrode holder. The liquid reagents were introduced to the electrode system and electrochemical analysis was performed.

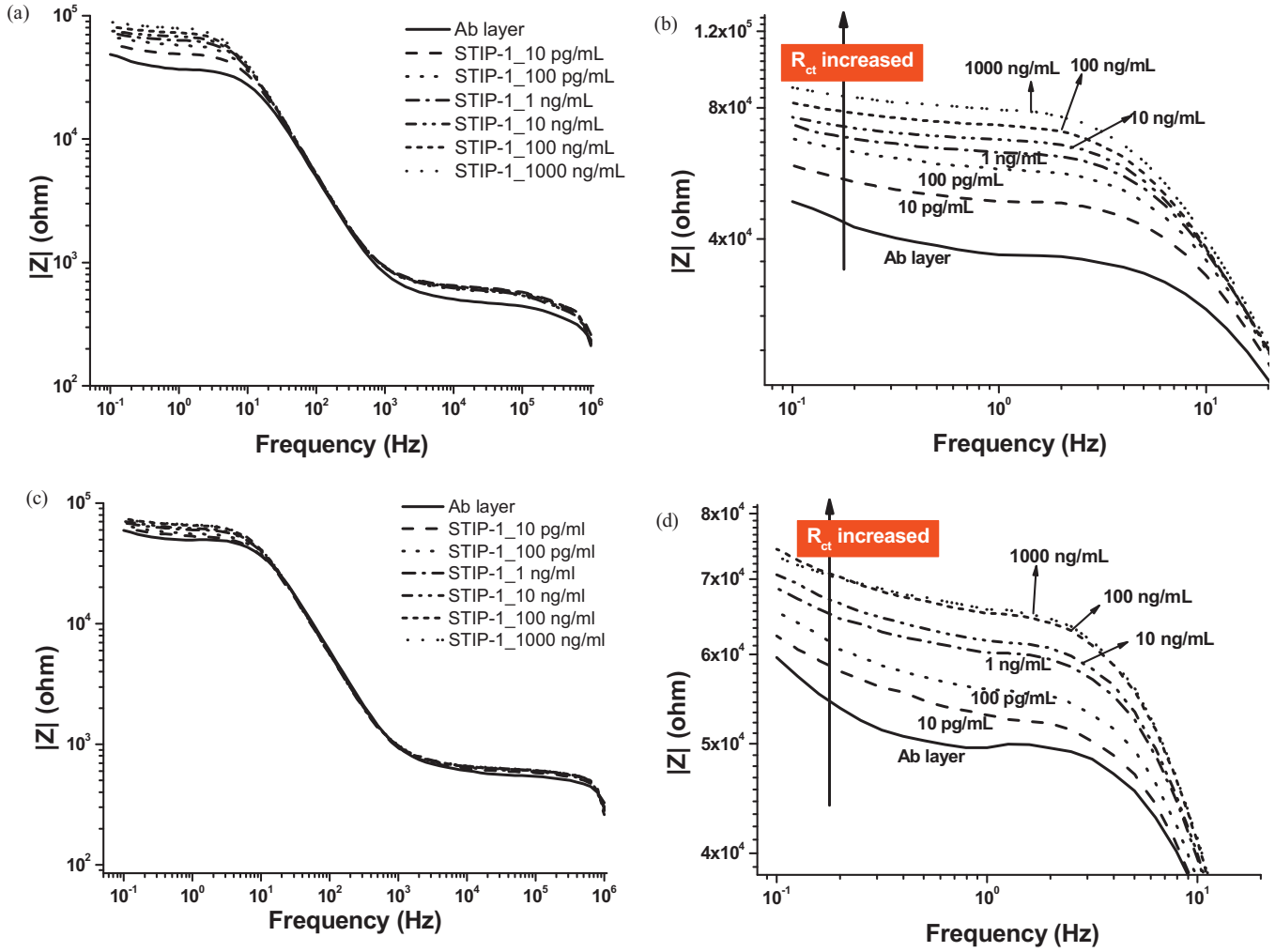

Fig. 3. Bode plot for binding of STIP-1 to the immunolayer on the electrodes. The applied potential was set to 50 mV against an Ag/AgCl reference electrode. The frequency range was 0.1 Hz to 1 MHz. (a) The small graph in the figure shows the bode plot of NWA electrode. (b) The large graph is the expansion of the frequency region from 0.1 Hz to 20 Hz as designated on the small bode plot. (c) The bode plot of bare electrode. (d) Expansion of the frequency region from 0.1 Hz to 20 Hz as designated on the (c).

3. Results and discussion

3.1. Wafer-scale NWA patterning

Fig. 1(b) shows the 57 uniform and well-fabricated NWA electrodes on a 6-inch Si wafer fabricated by KrF stepper semiconductor process for industrial application. The size of a single NWA sensor was 21 mm × 10 mm. Each sensor consisted of two NWA with a size of 4 mm × 2 mm. Each NWA structure had a diameter of 500 nm with an interwell spacing of 200 nm.

3.2. Electrochemical impedimetric measurements of affinity binding to NWA electrode

Fig. 2 shows the Nyquist plot for NWA electrodes using STIP-1 as a model analyte. In a nyquist representation, the real component of the complex impedance is shown on the *x*-coordinate, and the imaginary component on the *y*-coordinate. The semicircular plot in Fig. 2(a) and (b) is typically seen in simple electrochemical systems. The diameter of the semicircle corresponds to the charge transfer resistance, which is inversely related to the charge transfer rate at the interface (Bard and Falukner, 2001). By using impedance analysis program (*Z* plot), we applied the modified randles circuit (R_{sol})(C_{dl}[$C_{ps}R_{ct}$]) to experimental data, and calculate the R_{ct} component. R_{sol} is the solution resistance, C_{dl} is the double layer capacitance, C_{ps} is the pseudo capacitance and R_{ct} is the charge transfer resistance.

We determined the charge transfer resistance (R_{ct}) of the anti-STIP-1 antibody layer to be 36.96 kΩ. After antigen treatment, the R_{ct} was determined to be 48.39 kΩ, 57.26 kΩ, 62.98 kΩ, 68.26 kΩ, 75.13 kΩ and 80.70 kΩ, for 10 pg/mL, 100 pg/mL, 1 ng/mL, 10 ng/mL, 100 ng/mL, and 1000 ng/mL STIP-1, respectively, (Fig. 2(a)). To compare the sensitivity of the NWA biosensor with that of other electrode-based biosensors, the same treatments were applied to a bare electrode without NWA. For the bare electrode (Fig. 2(b)), the base R_{ct} was 52.52 kΩ, which represents an increase of 42% over the base R_{ct} of the NWA electrode. The R_{ct} values for 10 pg/mL, 100 pg/mL, 1 ng/mL, 10 ng/mL, 100 ng/mL and, 1000 ng/mL STIP-1 were 54.22 kΩ, 55.34 kΩ, 59.94 kΩ, 61.64 kΩ, 65.43 kΩ and, 65.83 kΩ, respectively.

The differences in the impedance spectra for each electrode before and after STIP-1 addition are shown in Fig. 2(c). For the bare electrodes, the impedance at low frequencies interfered with the measurement of the limit of detection (LOD). This low signal-to-noise ratio (S/N ratio) was caused by non-specific binding of STIP-1. It is reasonable to estimate an LOD of 1 ng/mL for the bare electrodes. The LOD was estimated to be 10 pg/mL or less for the NWA electrodes, which suggests a 100-fold improvement in the LOD

Table 1
Simulated values of R_{ct} and R_s after binding of STIP-1 to the immunolayer. Values were determined by fitting the measured data to an equivalent circuit, and calculating percent changes.

Concentration of STIP-1	R_s (kΩ)	Change (%)	R_{ct} (kΩ)	Change (%)
10 pg/mL	0.60	–	48.39	–
100 pg/mL	0.61	2.69	57.26	18.33
1 ng/mL	0.62	3.10	62.98	30.15
10 ng/mL	0.62	4.23	68.26	41.06
100 ng/mL	0.64	7.53	75.13	55.26
1000 ng/mL	0.65	8.78	80.70	66.77

when using EIS with NWA electrode. The sensitivity of the NWA impedimetric immunosensor was better for each analyte concentration tested when compared the sensitivity of the bare electrode sensor. Thereby, bare electrode has large area (4 mm × 2 mm) than NWA electrode (1.75 mm^2). Basically, large area electrodes provide the sensor with a good signal-to-noise ratio because binding site is increased. But, in this study, NWA's S/N ratio is higher than bare electrode although NWA has smaller area than bare electrode. The signal for the negative control (without antibody) was not significant, which further supports our finding of high specificity for the NWA electrodes.

Based on these results, the electrochemical impedimetric immunosensors using NWA electrodes can be applied for label-free detection, with low levels of non-specific binding. Because NWA are optimal for the selective docking of single molecules, they reduce non-specific binding and enhance electrochemical responses. Therefore NWA have high sensitivity and selectivity as well as very low LOD.

3.3. *Electrochemical impedimetric analysis of STIP-1 binding to the NWA sensor*

As previously mentioned, we applied modified randles circuit to fit our experimental data. In the Bode plot, shown in Fig. 3, there is a change of the magnitude of the impedance ($|Z|$) at the low frequency (<100 Hz). And signal in this region is dominated by the dielectric behavior of the electrode. For the high frequency region (>10^4 Hz), the resisitive region appears and resistance in the solution determines the signal (Yang et al., 2004). In low frequency region, the magnitude of impedance increases with increaing STIP-1 concentration, but the impedance change is negligible in high frequency region. Table 1 shows changes in the high-frequency-impedance signals (R_s) and the low-frequency-impedance signals (R_{ct}) for varying STIP-1 concentrations. The R_{ct} incresed by 66.77% for 1000 ng/mL STIP-1, over the value obtained with 10 pg/mL STIP-1. In contrast, the R_s incresed by only 8.78%, which demonstrate that R_s does not reflect the STIP-1 concentration. That means, higher concentrations of STIP-1, cause increased binding of STIP-1 to the anti-STIP-1 antibody layer, which creates a denser and thicker electrical isolation layer [Lee et al., 2009]. And these properties was observed in low frequency region by EIS. Changes of the double layer properties at lower frequency will be more dramatic than the changes in the solution resistance at higher frequency region.

4. Conclusion

A highly sensitive electrochemical impedimetric immunosensor based on wafer-scaled NWA was successfully applied for quantitative detection of STIP-1, which is a biomarker for ovarian cancer. At low frequencies, binding of STIP-1 to the immunoaffinity layer on the NWA electrodes resulted in large changes in impedance, and this effect was not observed for high frequencies. Thus, double-layer properties are more useful than solution resistance for qualifying STIP-1. From the NWA electrodes, we calculated the change in R_{ct} and estimated LOD for STIP-1 to be 10 pg/mL which represents a ≥100-fold improvement over bare electrodes. Electrochemical impedimetric NWA biosensor can also be applied for label-free detection without non-specific binding by means of the selective docking of immobilized antibodies. These properties provide high sensitivity and selectivity for wafer-scaled NWA sensor. The results also show the advantages of using NWA over large areas to improve performance and decrease costs.

Acknowledgements

This research was supported by the Basic Science Research Program of the National Research Foundation of Korea (NRF), funded by the Ministry of Education, Science and Technology (2008-0061862). And also supported by the National Science Foundation Nanoscale Science and Engineering Center (NSEC) for High-Rate Nanomanufacturing (grant no. 0832785).

References

Bard, A.J., Falukner, L.R., 2001. Electrochemical Methods Fundamentals and Applications, 2nd ed. John Wiley & Sons, New York.
Berggren, C., Bjanarson, B., Johansson, G., 2001. Capacitive biosensors. Electroanalysis 13, 173–180.
Chen, J., Zhang, J., Yang, H., Fu, F., Chen, G., 2010. A strategy for development of electrochemical DNA biosensor based on site-specific DNA cleavage of restriction endonuclease. Biosens. Bioelectron. 26, 144–148.
Daniels, J.S., Pourmand, N., 2007. Label-free impedance biosensors. Electroanalysis 19, 1239–1257.
Diouani, M.F., Hlali, S., Hafaid, I., Hassen, W.M., Snoussi, M.A., Ghram, A., Jafferzic-Renault, N., Abdelghani, A., 2008. Miniaturated biosensor for avian influenza virus detection. Mater. Sci. Eng. C. 28, 580–583.
Felice, J.S., Valentinnuzzi, M.E., Vercellone, M.I., Madrid, R.E., 1992. Impedance bacteriometry: medium and interface contributions during bacterial growth. IEEE Trans. Biomed. Eng. 46, 1310–1313.
Felice, C.L., Valentinuzzi, M.E., 1999. Medium and interface components in impedance microbiology. IEEE Trans. Biomed. Eng. 46, 1483–1487.
Hause, L.L., Komorowski, R.A., Gayon, F., 1981. Electrode and electrolyte impedance in the detection of bacterial growth. IEEE Trans. Biomed. Eng. 28 (5), 403–410.
Hanien, M., Diouani, M.F., Helali, S., Hafaid, I., Hassen, W.M., Renault, N.J., Ghram, A., Abdelghani, A., 2008. Immobilization of specific antibody on SAM functionalized gold electrode for rabies virus detection by electrochemical impedance spectroscopy. Biochem. Eng. J. 39, 443–449.
Kim, J.M., Jung, H.S., Park, J.W., Oka Yjkimasa, H., Lee, H.Y., Kawai, T., 2005a. Spontaneous immobilization of liposomes on electron-beam exposed resist surfaces. J. Am. Chem. Soc. 127, 2358–2362.
Kim, Y.S., Jung, H.S., Matsuura, T., Lee, H.Y., Kawai, T., Gu, M.B., 2005b. Electrochemical detection of 17beta-estradiol using DNA aptamer immobilized gold electrode chip. Biosens. Bioelectron. 22, 2525–2531.
Kim, P., Lee, B.G., Lee, H.Y., Kawai, T., Suh, Y., 2008. Molded nanowell electrodes for site-selective single liposome arrays. Adv. Mater. 20, 31–36.
Lee, H.Y., Park, J.W., Kim, J.M., Jung, H.S., Kawai, T., 2006. Well-oriented nanowell array metrics for integrated digital nanobiosensors. Appl. Phys. Lett. 89, 113901–113903.
Lee, J.K., Noh, G.H., Pyun, J.C., 2009. Capacitive immunoaffinity biosensor by using diamond-like carbon (DLC) electrode. Biochip. J. 3, 287–292.
Mathebula, N.S., Pillay, J., Toschi, G., Verschoor, J.A., Ozomena, K.I., 2009. A potential impedimetric immunosensing platform for active tuberculosis. Chem. Commun., 3345–3347.
Primiceri, E., Chiriaco, M.S., Ionescu, R.E., D'Amone, E., Cingolani, R., Rinaldi, R., Maruccio, G., 2009. Development of EIS cell chips and their application for cell analysis. Microelectron. Eng. 86, 1477–1480.
Wang, T.H., Chao, A., Tsai, C.L., Chang, C.L., Chen, S.H., Lee, Y.S., Chen, J.K., Lin, Y.J., Chang, P.Y., Wang, C.J., Chao, A.S., Chang, S.D., Chang, T.C., Lai, C.H., Wang, H.S., 2010. Stress-induced phosphoprotein 1 as a secreted biomarker for human ovarian cancer promotes cancer cell proliferlation. Mol. Cell. Proteomics 9, 1873–1884.
Yang, L., Li, Y., Griffis, C.L., Johnson, M.G., 2004. Interdigitated microelectrode (IME) impedance sensor for detection of viable *Salmonella typhimurium*. Biosens. Bioelectron. 19, 1139–1147.
Yu, X., Lv, R., Ma, Z., Liu, Z., Hao, Y., Li, Q., Xu, D., 2006. An impedance array biosensor for detection of multiple antibody–antigen interactions. Analyst 131, 745–750.